

Trajectory correction studies for the CNGS proton beam line

W. Herr and M. Meddahi, SL Division, CERN, 1211-Geneva 23

Abstract

The aim of this study was to check the performance of the presently proposed trajectory correction scheme for the CNGS proton beam line. We would like to answer the following questions: Is the proposed scheme sufficient ? Can we save some correctors or monitors ? What happens if something goes wrong (i.e. correctors or monitors are faulty) ? We also attempt to identify possible critical scenarios which may not be visible in a purely statistical analysis. This part of the analysis is based on common sense and largely on the experience from SPS and LEP trajectory and orbit correction problems.

Geneva, Switzerland

16th May 2002

1 CNGS proton beam

The CERN Neutrinos to Gran Sasso (CNGS) project, presently under construction, is a collaboration between CERN and the Gran Sasso Laboratory of INFN in Italy, with the aim to study neutrino oscillations in a long base-line experiment [1, 2, 3]. An intense proton beam is extracted from the SPS accelerator at a nominal energy of 400 GeV, transported through a 840 m long proton transfer line, before impinging on a graphite target. Secondary particles created in the target are directed towards Gran Sasso and will, in turn, decay in flight, producing mostly ν_μ . These neutrinos, which hardly interact with matter, will travel 730 km through the earth towards the Gran Sasso laboratory, where the appearance of ν_τ will be studied. The general CNGS layout is shown in Fig.1. The proton beam is extracted from the SPS

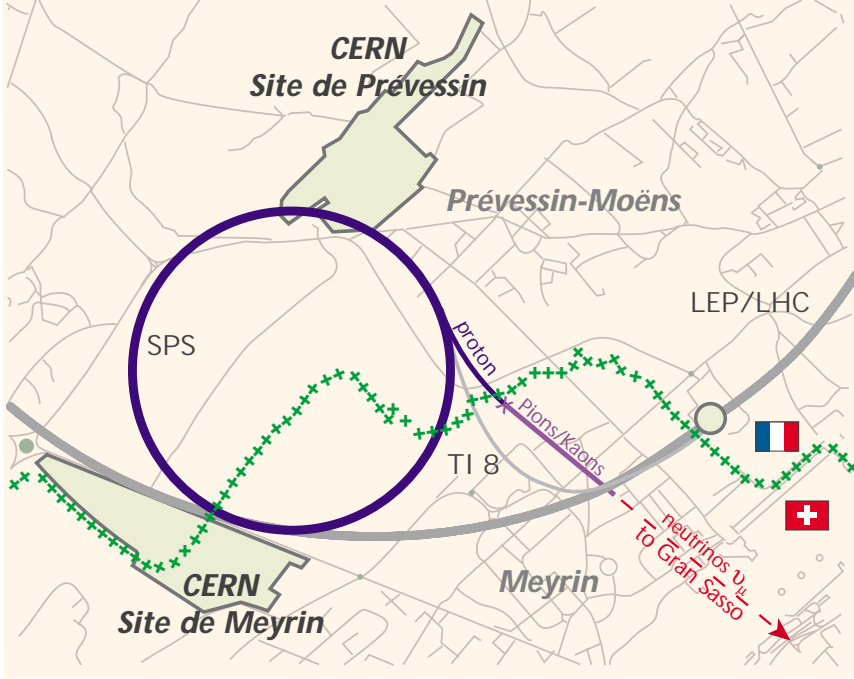


Figure 1: Overview of the CNGS Layout.

in LSS4 at 400 GeV, in two consecutive $10.5 \mu\text{s}$ fast extractions, in a 6 s cycle. The nominal intensity per extraction is 2.4×10^{13} p/extraction with an upgrade phase to 3.5×10^{13} p/extraction. The CNGS project benefits from the extensive work done for the LHC fast extraction as it will be using the same channel as the LHC beam in LSS4, as well as a common beam line in TT40 over about 200 m [4, 5, 6]. In order to steer this intense beam through the proton line (called TT41), beam position monitors and dipole correctors are positioned along the line. The relatively tight aperture requires a precise control of the trajectory. The strongest aperture constraint comes from the main dipoles (MBG) [7]. Their nominal gap height of 37 mm results in a full physical aperture for the beam of 31.4 mm as shown in Tab.1. The

	size [mm]
Nominal gap height	37
Mechanical tolerances	± 0.2
Vacuum tube thickness incl. tolerances and insulation foils	2×1.7
Sagitta (hang-through)	± 0.5
Misalignment	0.8
Remaining full physical aperture A	31.4

Table 1: Physical vertical aperture in the main dipole MBG.

maximum allowed trajectory excursion E_{max} after correction is derived using the formula :

$$\frac{A}{2} = (5\sigma + D\Delta p/p)k_{\beta} + E_{max}\sqrt{\beta/\beta_{max}} \quad (1)$$

with A the full physical aperture (31.4 mm for the MBG vertical aperture), k_{β} the optical mismatch (1.1), $\Delta p/p$ the momentum spread 0.12% and $\sigma = \sqrt{\beta * \epsilon}$. The nominal emittance (at 400 GeV) is 28.1 nm. This leads to a maximum tolerable vertical excursion of 5.2 mm at the MBG dipoles following a QD. The tightest aperture is located between QTG4118 and QTG4119 (large vertical β function) with a value of 3.5 mm. This location must be well monitored.

It is felt that 10% for the β -beating ($k_{\beta} = 1.1$) may be too optimistic and performing the same calculation with 20% β -beating provides a maximum tolerable trajectory excursion of 4.3 mm. The available aperture between QTG4118 and QTG4119 is now reduced to 2.7 mm.

Finally it has to be pointed out that the β_{max} values are taken to be 108.6 m and 106.3 m in the horizontal and vertical plane, respectively. This case corresponds to the maximum β value taken in the FODO cell. If we take these maximum values in the whole beam line, the values are respectively 345.8 m and 162.5 m, which would give a more favorable allowable trajectory excursion (25% more).

In summary, it was decided for this study to take the following parameters: 5σ beam, β -beating of 20%, β_{max} values taken in the FODO cells. The resulting maximum acceptable excursion is then 4.3 mm with a worst case between QTGF4118 and QTGD4119 where good beam monitoring should be available.

2 Beam line errors

The following errors were included in the calculation of the trajectory: quadrupole displacement, beam position monitor error, main dipole field and tilt errors, and finally injection errors (in position and angle). The magnitude of these errors is similar to the ones defined in earlier work done for the LHC transfer lines [8, 9].

2.1 Main quadrupole (QTG) errors:

All main quadrupoles (QTG, [10]) are allowed to be displaced in the horizontal and vertical plane. The possible displacements are approximated by a Gaussian distribution with a σ of 0.2 mm. This distribution is cut at $\pm 3\sigma$. The origin of these displacements is the resolution during the alignment, and the deformation of the ground.

2.2 Monitor errors:

The errors in both planes are represented by a flat random distribution of ± 0.5 mm. These errors stem from electrical, mechanical and alignment errors.

2.3 Main dipole (MBG, MBGT) field error:

There are 73 main dipole magnets in the line for which field dipole errors will contribute to a deviation from the reference trajectory. Errors in the few dipoles of other type (MBHC, MBHA, MBSG) are neglected. The specification requires that each magnets stays within $\pm 5.0 \cdot 10^{-4}$ of the average field [7]. The resulting distribution of the deflections is assumed to be Gaussian with a σ of $2.0 \mu\text{rad}$ cut at $\pm 2\sigma$, which corresponds approximately to $\pm 5.0 \cdot 10^{-4}$ of the nominal deflection of 8 mrad.

2.4 Main dipole tilt errors:

Magnet distortions around the beam axis (i.e. the direction of the field lines varies along the magnet length) are possible and should be taken into account. This tilt results in additional vertical deflections

depending on the tilt angle whereas the normal horizontal deflection stay almost unchanged. During alignment, the resolution of each measurement done along the magnet to measure its tilt will be 0.2 mrad. For our simulations, the tilt errors are assumed to be distributed like a Gaussian with a σ of 1.6 μrad (0.2 mrad*8mrad nominal horizontal deflection), cut at $\pm 4 \sigma$.

2.5 Injection errors:

Injection errors are taken to be Gaussian with an injection position error with a σ of 0.5 mm and an injection angle error with a σ of 0.05 mrad, both cut at $\pm 2 \sigma$.

3 Correction algorithm and strategies

The correction of a trajectory serves two different aspects: to steer the beam through the line in the first place, and after this beam threading, to keep the excursions as small as possible. The measurement of a trajectory is more difficult than to measure a closed orbit since only a single pass is measured and usually with lower intensity. Correction algorithms should be able to cope with faulty measurements and monitors. While the initial steering is typically done with low intensity pilot beams, care must be taken to control the trajectory of a high intensity beam, and the CNGS beams will be operated at the highest intensities available. The first choice for the correction is therefore a least squares method, ideally with a small number of correctors to be less sensitive to bad measurements. For this study we have used the MICADO algorithm which is widely spread and was successfully used in the SPS and LEP. The program we have used is the newly developed MAD-X program[11], the successor of MAD8. For the present study MAD-X is well suited since it has several features not available in MAD8:

- Correction of a trajectory with a modified version of MICADO.
- Consistent treatment of monitor errors within the correction program.
- Possibility to disable monitors randomly, using a specified fault probability.
- Loops in the MAD-X input structure allow accumulation of statistics while saving all relevant results.
- Easy access to the correction data for post-analysis.
- Last but not least full access to the algorithms and procedures in MAD-X.

4 First evaluation of the present scheme

4.1 Description of the present trajectory correction scheme

In 2000, an extensive trajectory study for the LHC transfer lines was performed [9]. This trajectory study program was also applied to the CNGS proton beam line and it was tentatively concluded that to stay within the given aperture, two consecutive quadrupoles per plane out of three should be equipped with monitors (BPM) and correctors (referred as a 2-in-3 scheme) [12]. The scheme is summarized in Tab.2 and Tab.3 and is referred in this note as "present scheme".

monitor:	m	m		m	m		m	m			m	m	m
corrector:	c		c	c		c	c		c		c	c	
Quadrupole: (QTG41XX)	02	04	06	08	10	12	14	16	18	20	22	2423	2446

Table 2: *Pattern of the monitors and correctors in the horizontal plane.*

monitor:	m	m		m	m		m	m		m	m		m	m	m
corrector:			c	c		c	c		c	c		c		c	
Quadrupole: (QTG41XX)	01	02	03	05	07	09	11	13	15	17	19	21	23	2423	2446

Table 3: *Pattern of the monitors and correctors in the vertical plane.*

The corrector dipoles used in the line are new magnets (MDG) dedicated for the CNGS proton line, which have not yet been designed. New corrector magnets (called MDM in SPS naming convention and MCIA in LHC naming convention [13]) designed for the LHC transfer lines and recuperated SPS dipole corrector magnets (MDS) are also used. Their characteristics are summarized in the Tab.4.

	MDSH/V	MDGH/V	MDMH/V
Length [m]	0.7	0.548 flange to flange	0.450
Nominal \int Bdl [Tm]	0.77	0.107	0.12
Bending angle at 400 GeV [μ rad]	577	80	90
Aperture [mm]	70	45	32

Table 4: *Corrector's characteristics.*

4.2 General considerations and π bumps

In principle, the trajectory in a regular lattice can be corrected with a 2-in-3 corrector scheme. A similar reasoning was used for the proposal to install a 2-in-3 corrector scheme in the LEP arcs. However, in LEP all defocusing quadrupoles were equipped with horizontal and vertical monitors to make such a scheme functioning. This is not the case for the CNGS proton beam line as proposed today. Furthermore, in CNGS the phase advance per cell is close to $\pi/2$ in both planes, therefore it is possible to produce so-called π -bumps that may not be visible because the trajectory is heavily under-sampled. To illustrate this, the displacement of two vertical quadrupoles was simulated. In Fig.2 the resulting trajectory is shown at all beamline elements. In Fig.3 (left) it is shown how the trajectory actually appears on the presently proposed beam position monitors of the line. The maximum excursion of the bump is not visible and therefore not correctable. The result of a trajectory correction using this beam position

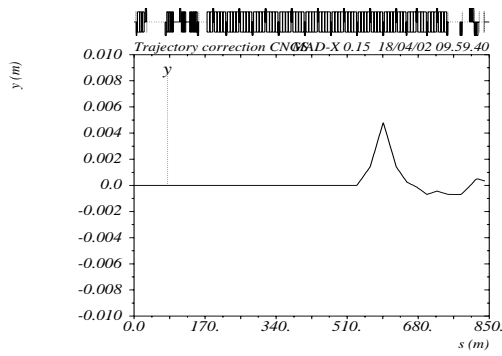


Figure 2: Vertical bump in all machine elements.

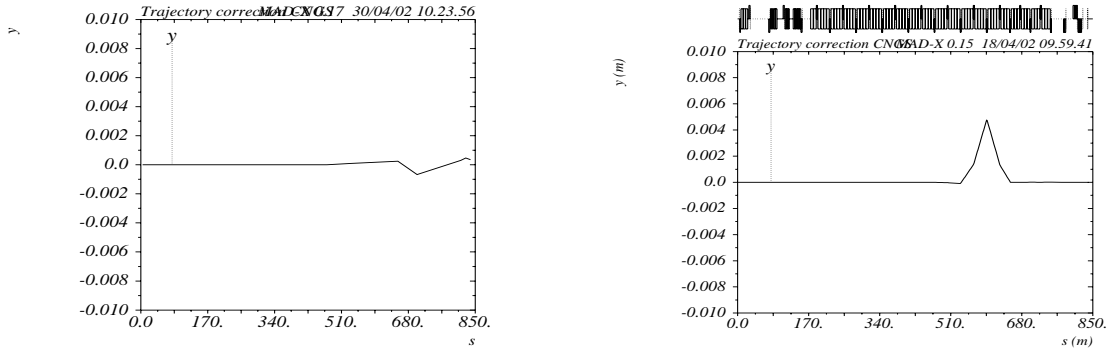


Figure 3: Vertical bump with present monitoring scheme (left) and after correction in all machine elements (right).

monitor information is shown in Fig.3 (right), again by looking at all elements of the whole beamline. The bump produced by the displacement is not corrected because it is not visible for the correction procedure due to the missing monitor. Although it is possible in MAD-X to deal with such a case, in practice a correction program in the control room uses only the beam position monitor information. An extra monitor (near quadrupole 15) was added in Fig.4 (left) to the present scheme at the position of the bump (to be compared with Fig.3 (left)). This effect of this additional BPM on the trajectory correction is shown in Fig.4 (right), again by looking at all elements of the whole beamline (to be compared with Fig.3 (right)). The maximum trajectory excursion is now reduced at the expense of two smaller bumps. This is because missing correctors in the region of the bump do not allow to flatten the entire trajectory.

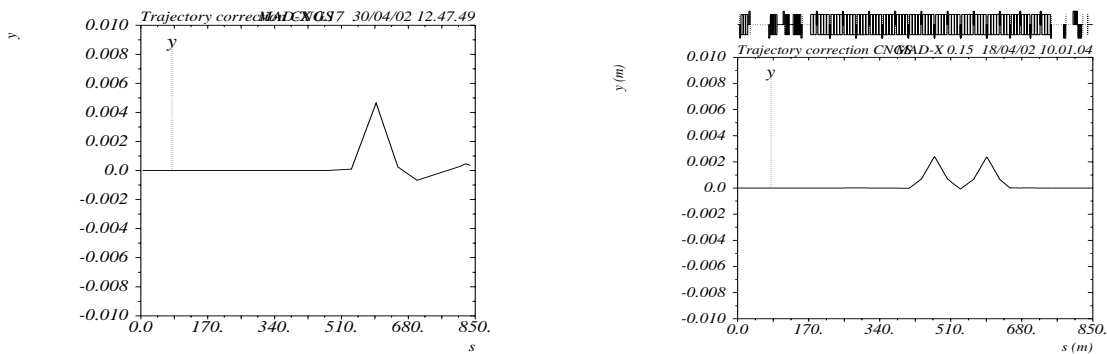


Figure 4: Vertical bump with one additional monitor and after correction with modified correction scheme.

Additional correctors were added in Fig.5. Now the trajectory can be corrected in the entire range.

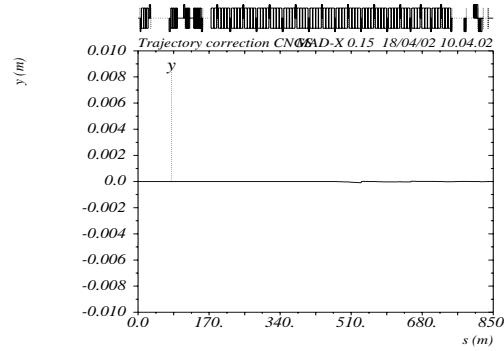


Figure 5: Vertical bump after correction with additional monitor and additional correctors.

The effect on the trajectory of two neighbouring, displaced quadrupoles with a phase advance of π between them, can formally be separated into two distinct structures: a local bump and the result of a single kick. It can easily be seen that in 50% of all cases the bump structure will materialize as a local, invisible (for BPMs) trajectory excursion, that is not correctable. Furthermore, subsequent trajectory corrections can enhance this 'invisible bump' more and more unless special precautions are taken. A prominent example for such a case is again the LEP trajectory in the interaction region.

To summarize: for the original scheme one can construct scenarios where the trajectory excursions are largely outside the allowed range without the possibility of measurement and thus correction. A solution would be either to add monitors and correctors or to change the phase advance to ideally 60° per cell or at least 80° .

Studies on changing the phase advance reveal that it is impossible to zero the dispersion functions at the end of the line, at the target. Moreover, the values of the dispersion along the line increase, which, together with an increase of the β functions (reduction of the phase advance), lead to a reduction of the available aperture. This is not surprising as the design of the CNGS proton beam line has been performed in view of minimizing the cost, i.e. reducing the beam line length as much as possible. Changing the phase advance, while fulfilling the optical constraints, requires to lengthen the line, and therefore to change the beam line geometry. This is not feasible at this stage of the project. Another solution would be to add more quadrupoles in the line, each of them equipped with independent power supplies. However there is no available position in the regular cell to add them and the cost of these additions would have been much higher than adding some beam position monitors in the line or equipping the existing ones with a readout in both planes.

Finally, it has also to be reminded that the phase advance of 90° was chosen since this is the optimum choice to provide the maximum beam acceptance (for a round beam)[14].

4.3 One crucial monitor missing

Standard trajectory corrections were applied to simulate trajectories with all errors as specified in section 2, using the present scheme to get a first picture. It was immediately found that a monitor was missing in the present scheme (BPH4120, see Tab.2). A reasonable trajectory correction is basically impossible without this monitor. In the following studies, the monitor (BPH4120) was therefore inserted.

4.4 Possible use of bending magnets as correctors

The bending magnets MBHC and MBHA can be used as correctors in addition to the dedicated correction magnets. This helps to avoid creating bumps at the beginning of the line and to reduce the required strength of other correctors.

5 Trajectory simulation results

5.1 Efficiency studies of specific correctors

In this first part we do not take into account possible injection errors. They will be treated separately in a later section. A typical trajectory (i.e. one of the worst) before and after correction is shown in Fig.6. In Tab.5 we summarize the maximum rms and maximum trajectory excursion before and after

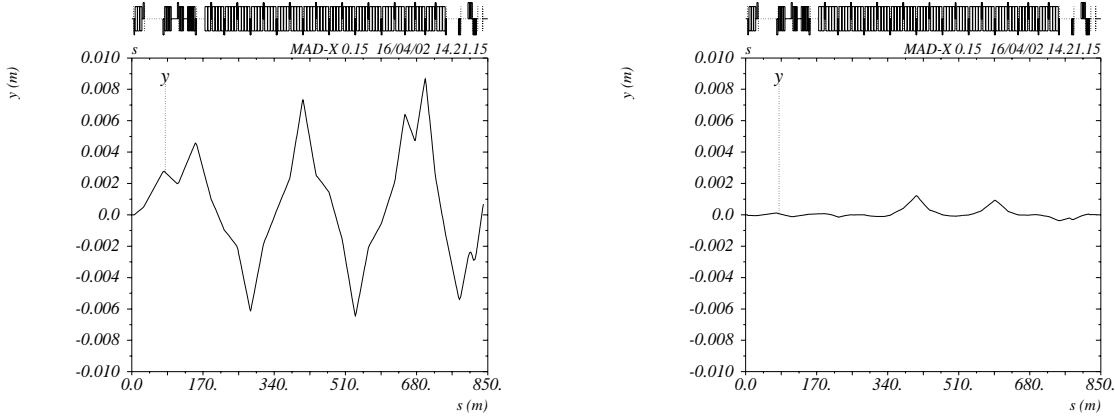


Figure 6: Vertical trajectory before and after correction.

	RMS max (mm)	trajectory max (4.3 mm max allowed) (mm)
X before	3.36 (3.54)	7.33 (13.71)
X after, 5 correctors used	1.12 (1.08)	3.38 (5.10)
X after, all correctors	0.75 (0.77)	2.09 (4.18)
X after, all correctors, without MDMH4001	1.34 (1.32)	4.03 (4.55)
Y before	3.50 (3.20)	8.84 (9.01)
Y after, 5 correctors used	1.04 (1.14)	3.00 (4.40)
Y after, all correctors	0.31 (0.80)	0.78 (3.42)
Y after, all correctors, without MDSV4003	0.37 (0.86)	1.20 (3.42)

Table 5: Results of trajectory corrections with all errors. Numbers correspond to values at monitors. Values in parenthesis correspond to values at all machine elements. Boldface indicates present scenario.

correction of 3000 simulated trajectories¹. For the correction we suppose the use of two sets of correctors (either restricted to 5 or using all available correctors). The comparison shows the importance of a sufficient number of correctors. We also study the importance of two selected correctors: MDMH4001 and MDSV4003. We give both, the displacements at the monitors as well as in all machine elements. Looking at all machine elements, the corrected trajectories are mostly within the required limits, although with little margin. Exceptions where the trajectory is outside the permissible limit we get when fewer correctors are used or the corrector MDMH4001 is omitted. We find that the discrepancy between the two numbers is much larger in the vertical than in the horizontal plane. This is due to the different phase advance per cell in the two planes. It is 84.5° in the horizontal and 89.9° in the vertical

¹This number looks a bit excessive and it certainly is. However this study was also used to test the stability of MAD-X and we have therefore pushed it beyond the necessary limits

	Strength max (μrad)	Phase (2π rad)		Strength max (μrad)	Phase (2π rad)
MDMH4001	101.2 (70.0)	0.0708	MDMV4000	35.4	0.0050
MDMBHC	- (42.0)	0.1230	MDSV4002	30.5	0.1148
MDMBHA	- (35.0)	0.3495	MDGV4103	31.6	0.5868
MDGH4102	33.5	0.7165	MDGV4105	37.5	0.8368
MDGH4106	32.2	1.1865	MDGV4109	32.3	1.3363
MDGH4108	57.4	1.4215	MDGV4111	46.6	1.5862
MDGH4112	33.5	1.8914	MDGV4115	32.0	2.0857
MDGH4114	39.0	2.1263	MDGV4117	48.4	2.3249
MDGH4118	37.1	2.5268	MDGV4121	309.0 (-)	2.6565
MDSH4122	83.0	2.9949	MDSV4121	228.0 (37.9)	2.7304
MDSH4124	197.4	3.0360	MDSV4124	155.0 (92.0)	3.0003

Table 6: Correctors' phases and required strengths for trajectory correction with nominal errors. Left side for horizontal and right side for vertical plane.

plane. The possibility for an uncorrectable π -bump is therefore much larger in the vertical plane. This demonstrates very clearly that for such a phase advance what you see is **not** what you get. The required corrector strengths were recorded for all corrections and the maximum corrector strength used for each corrector is shown in Tab.6. The maximum needed corrector strengths remain below $60 \mu\text{rad}$, with a few exceptions: the MDMH4001 at the beginning of the line was as large as $101 \mu\text{rad}$ and the correctors at the end of the line (sequence number larger than 20) can go as high as $200 \mu\text{rad}$. The strength required for the MDMH4001 is therefore slightly higher than its maximum value (Tab.4). To prove that the re-

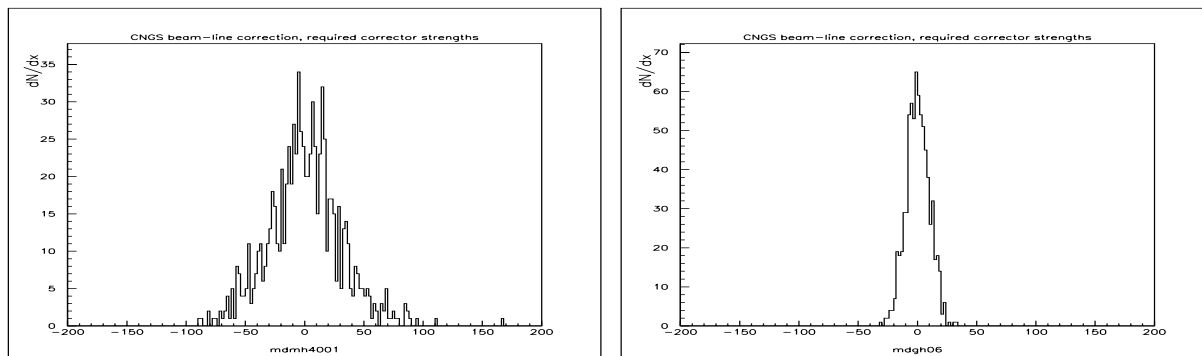


Figure 7: Distribution of required strength for correctors MDMH4001 and MDGH4106

quired strength is not a fluctuation but rather a feature of the scheme, we show in Fig.7 the distribution of strengths for 3000 corrections of the correctors MDMH4001 and MDGH4106. The maximum strengths are clearly not a single fluctuation but the tails of a wider distribution. In Tab.5 we have also shown the results one obtains *without* this corrector and the quality of the correction is significantly worse, up to a point where it is close to the maximum allowed excursion. The use of the two bending magnets MBHC and MBHA as additional correctors reduces the required strength to about $70 \mu\text{rad}$ (values in Tab.6 (left) in parenthesis). Whether this possible limitation of the correction strength of the corrector MDMH4001 is a potential problem is discussed in the next section.

The corrector MDSV4003 however, seems to be much less critical and we see no reason why it cannot be suppressed. In all following studies it is removed from the correction scheme.

The figures in parenthesis in Tab.6 (right) should be understood as follows: The correctors MDGV4121

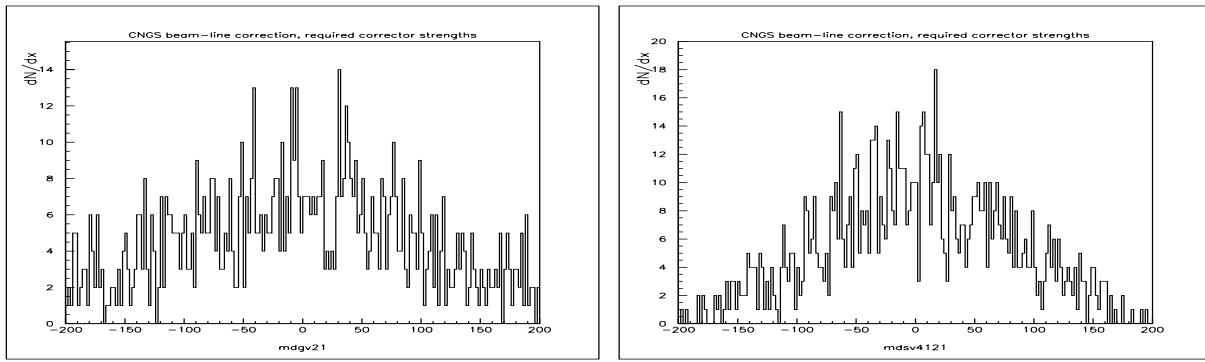


Figure 8: Distribution of required strength for correctors MDGV4121 and MDSV4121

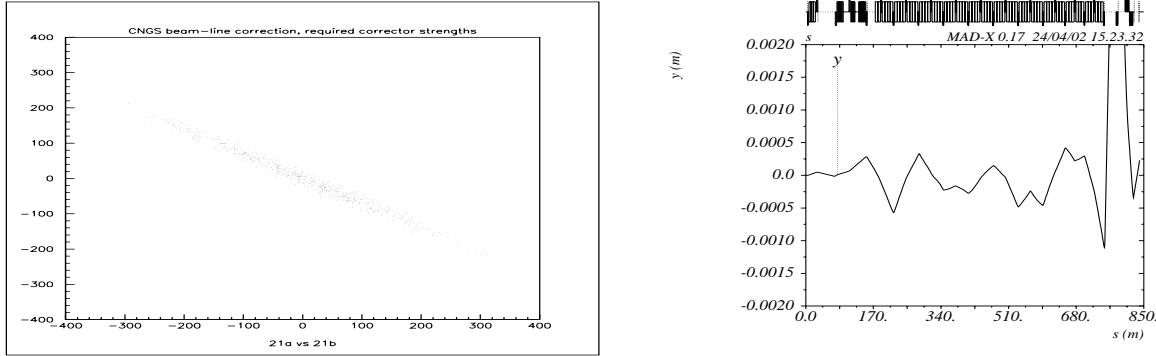


Figure 9: Correlation between correctors MDGV4121 and MDSV4121 and resulting trajectory

and MDSV4121 are very close without a monitor between them. As a result they can work "against" each other. The strength distributions of these correctors are shown in Fig.8. Both reach rather high values when they are naively used together. In Fig.9 we show the correlation between the two correctors as well as a resulting trajectory (in all machine elements). At around 770 m, the peak excursion is not visible on the monitoring system and therefore not visible on the control room screens. The anti-correlation is almost perfect, i.e. one of the correctors should be removed. From Fig.9 it can be guessed how often such a pathological situation appears. In parenthesis in Tab.6 (right) we give the maximum strengths for the following correctors when the corrector MDGV4121 is omitted. The quality of the trajectory correction in the visible part is unaffected and the required strengths in the last two correctors is strongly reduced. We therefore strongly suggest to drop this corrector from the scheme.

5.2 Effect and correction of injection error

Both, the position and the angle of the beam may be wrong at injection from the SPS into the proton beam line. The resulting trajectories add linearly to the trajectories caused by the other imperfections. The correction system should be able to cope with such errors. The size of possible injection errors is specified in section 2.5. The correction of an error in the injection angle of $50 \mu\text{rad}$ is shown in Fig.10. Other errors can be ignored in this example since they would only affect the beam later in the beam line. Looking at the results, in particular the necessary strengths of the correctors, it shows that the wrong angle is practically always corrected by one or two correctors in each plane. Furthermore, and not surprisingly, the required strength is almost identical to the wrong angle. Therefore we need correctors that can handle strengths in the order of $100 \mu\text{rad}$ or more at the beginning of the line. In the vertical plane this is the corrector MDMV4000 that is thus slightly above the maximum strength ($90 \mu\text{rad}$). In the case

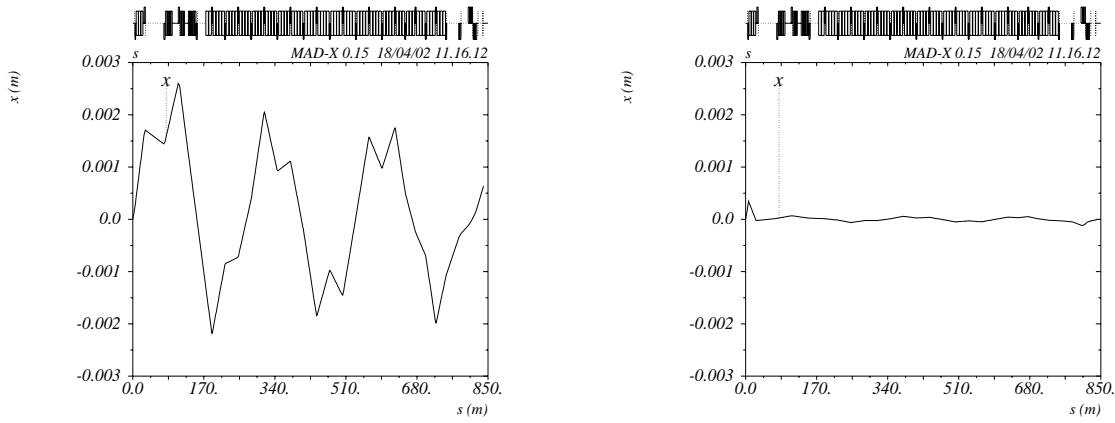


Figure 10: Example of a correction of the injection angle.

of a horizontal angle the strength must be provided by the corrector MDMH4001, which unfortunately is already pushed close to its limit by the requirements of the regular trajectory correction. Neither for the trajectory correction nor for the correction of the injection error it can be abandoned. We have tried to salvage at least part of the strength using a procedure that has been implemented successfully in the trajectory correction package COCU [15] used for the SPS and LEP. The results are shown in Tab.7.

Ceiling for maximum strength	Trajectory (max.) (mm)	RMS (mm)
0 % \equiv 0 μ rad	5.0	2.0
33 % \equiv 30 μ rad	3.3	2.0
50 % \equiv 45 μ rad	2.9	1.5
67 % \equiv 60 μ rad	2.4	1.2
100 % \equiv 90 μ rad	1.5	0.6

Table 7: Correction of injection error with ceiling for strength of MDMH4001.

When the correction is calculated, the strength computed for the MDMH4001 is cut at a predefined fraction of its maximum strength and remains fixed for all subsequent iterations where additional correctors are added and computed. The remaining part of the strength is then available for regular trajectory corrections. We show the maximum trajectory and r.m.s. after this correction procedure in Tab.7. It shows the results of such a procedure applied to the correction on an injection angle of 100 μ rad. They are rather encouraging and show that this strategy can be successfully used. Sharing the strength equally between the correction of an injection error and other beam line imperfections looks like an acceptable compromise.

6 If things go wrong ...

We have already demonstrated that the present scheme could be sufficient for 'reasonable' errors, but cannot handle particularly unlucky situations, such as π -bumps in places without monitors etc. This is only true when all elements are available and work according to the specifications. However, experience (e.g. LEP) shows that this is rarely the case. One has to expect faulty or unavailable correctors and monitors and in this situation the scheme deteriorates. In the following we restrict ourselves to study the effect of missing monitors.

6.1 Effect of monitors not working

The effect of missing monitors on the result of a correction can be disastrous. First, non-existing measurements can lead to large trajectory excursions in positions where they are not visible. Secondly, the correction algorithms do not work as well as expected. Missing measurements can either lead to an ill-defined problem that leads to the collapse of the correction procedure, or the correction procedure itself can produce 'bumps', i.e. large trajectory excursions in places without monitors. The creation of such bumps is not easily visible by the operator. Fortunately, the latter can be avoided by a smart correction procedure. However, the first problem leads to a reduced number of usable correctors and inevitably to a worse correction. In the following we have used a new feature in MAD-X, i.e. the possibility to disable beam position monitors randomly, given a probability for the fault. The results are shown in Tab.8.

	RMS max (mm)	trajectory max (mm)
X before	4.06 (3.42)	9.24 (13.06)
X after	1.36 (3.22) [2.1]	3.57 (11.93) [8.1]
Y before	3.23 (3.01)	7.66 (8.13)
Y after	1.28 (3.46) [2.2]	3.04 (12.97) [5.8]

Table 8: 2% of monitors randomly disabled, using 5 correctors. Nominal monitoring scheme.

Although only in some cases (2%) a monitor was considered faulty, the difference is quite significant. While the trajectory correction looks rather satisfactory considering only the monitors, it becomes a disaster in other, invisible parts of the machine (in parenthesis). In particular, invisible bumps are produced, mainly in the vertical plane, which make the maximum trajectory excursions larger after the correction. A procedure was applied to avoid **creating** bumps during the correction process and the results are shown in brackets in Tab.8. Although the result is now better, it is still unacceptable. This strong effect can easily be understood. In the Figs.11 and 12 we demonstrate the effect of one missing monitor on the measured trajectory generated by a single displaced quadrupole². The missing monitor is BPV4105 and because of the phase advance of $\pi/2$, two monitors are in positions where the trajectory is zero ($\leq 0.1 \mu\text{rad}$), thus providing no information. Because of this arrangement, not only a complete wavelength of the trajectory oscillation is invisible, but also all correctors within this wavelength become useless and a naive correction procedure will not find a good solution. Although strategies exist to improve the trajectory correction of such cases, (e.g. analyzing a set of trajectories with slightly different initial conditions), they are more involved and do not provide a turnkey solution. This could be used for the commissioning, but not for regular operation.

Inspecting the lattice, we observe that we could recover if all the BPM bodies presently foreseen in the beam line are equipped to measure the trajectory in both planes. In Fig.12 (right) we have therefore considered all available monitors equipped in both planes and show again the trajectory above, still omitting the monitor BPV4105. The structure of the bump is now visible again and the defect can be

²This example is not constructed: such cases appeared regularly during the simulations for Tab.8.

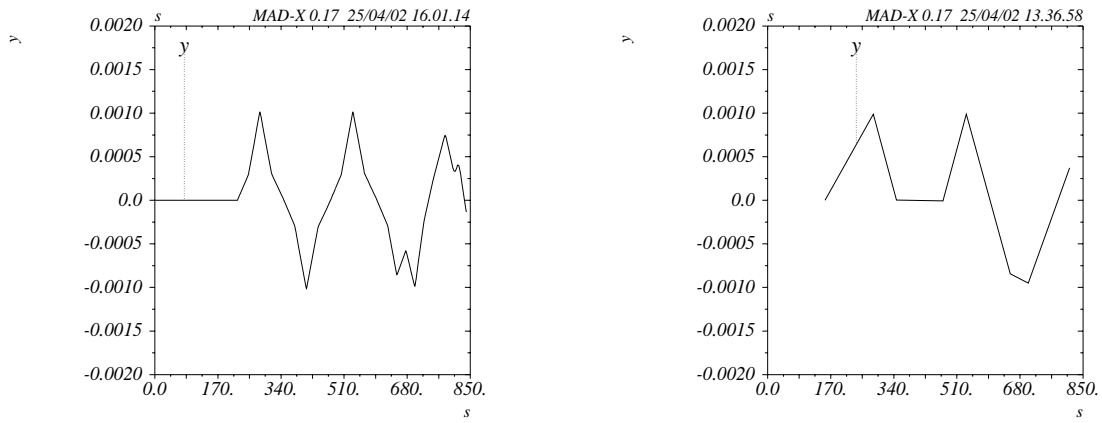


Figure 11: Measured trajectory at all beam line elements (left) and at existing monitors (right).

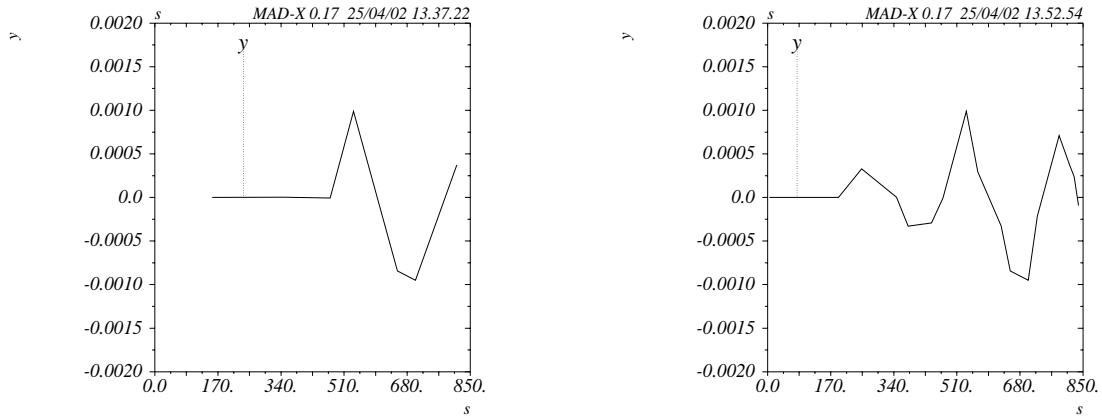


Figure 12: Measured trajectory with one monitor missing, using the existing monitors (left), and with all these existing monitors equipped in both planes (right).

corrected at its origin. An analysis with 3000 different trajectories using this modified scheme confirmed our expectation that the correction can be significantly improved. The results are shown in Tab.9. All corrected trajectories are now well below the allowed maximum, with a considerable margin. The results for the alternative scheme with monitors (one plane) at all quadrupoles are shown in Tab.10. The results are slightly worse. In Tab.11 we have again randomly disabled 2% of the available monitors, like for Tab.8. However, this time with all monitors for both planes, thus increasing the number of monitors and improving the sampling significantly. It should be noted that for technical reasons the sequence of random numbers for the simulations summarized in Tab.8 and the following tables is not the same and therefore the trajectories before correction are slightly different when the number of monitors is different. The quality of the correction is still fully satisfactory and according to the specifications. The corresponding results for all quadrupoles equipped with monitors is shown in Tab.12.

	RMS max (mm)	trajectory max (4.3 mm max allowed) (mm)
X before (BPM in both planes)	3.57 (3.58)	10.98 (15.02)
X after (BPM in both planes)	0.65 (0.65)	2.02 (2.68)
Y before (BPM in both planes)	3.24 (3.20)	7.50 (8.02)
Y after (BPM in both planes)	0.49 (0.62)	1.42 (2.52)

Table 9: Same as Tab.5 but with all monitors in both planes: Results of trajectory corrections with all errors. Numbers correspond to values at monitors. Values in parenthesis correspond to values at all machine elements.

	RMS max (mm)	trajectory max (4.3 mm max allowed) (mm)
X before (BPM at all quadrupoles)	4.15 (4.07)	7.79 (14.90)
X after (BPM at all quadrupoles)	0.60 (0.70)	2.02 (3.92)
Y before (BPM at all quadrupoles)	3.48 (3.28)	7.62 (7.62)
Y after (BPM at all quadrupoles)	0.61 (0.58)	2.20 (1.97)

Table 10: Same as Tab.5 but with all monitors at all quadrupoles: Results of trajectory corrections with all errors. Numbers correspond to values at monitors. Values in parenthesis correspond to values at all machine elements.

	RMS max (mm)	trajectory max (mm)		RMS max (mm)	trajectory max (mm)
X before	3.18 (3.57)	9.02 (15.02)	X before	3.18 (3.57)	9.02 (15.02)
X after	1.05 (1.19)	2.83 (5.26)	X after	0.62 (0.77)	2.02 (3.48)
Y before	3.24 (3.20)	7.50 (8.02)	Y before	3.24 (3.20)	7.50 (8.02)
Y after	1.00 (1.01)	3.10 (4.12)	Y after	0.49 (0.77)	2.02 (3.19)

Table 11: 2% of monitors randomly disabled, using 5 (left) and all correctors (right). All monitors for both planes.

	RMS max (mm)	trajectory max (mm)		RMS max (mm)	trajectory max (mm)
X before	4.16 (4.07)	7.79 (14.90)	X before	4.16 (4.07)	7.79 (14.90)
X after	1.11 (1.40)	3.10 (6.06)	X after	0.59 (1.38)	2.02 (5.83)
Y before	3.48 (3.28)	7.62 (7.62)	Y before	3.48 (3.28)	7.62 (7.62)
Y after	1.19 (1.13)	3.81 (3.85)	Y after	0.61 (0.67)	2.02 (3.28)

Table 12: 2% of monitors randomly disabled, using 5 (left) and all correctors (right). Monitors at all quadrupoles.

6.2 CONCLUSION

Based on a statistical analysis simulating 3000 different trajectories one could draw a first conclusion that in principle the trajectories can be corrected to the required precision with the proposed scheme. This confirms earlier findings [12]. However, the trajectory correction scheme provides no margin and unlucky situations can become showstoppers because of missing correction and monitoring elements. Whether the trajectory stays within the required aperture cannot be guaranteed since it is not visible in critical positions. Large injection errors may create problems since they reduce the availability of very important trajectory correctors significantly. A straightforward trajectory correction procedure cannot cope with such a situation. More sophisticated strategies like those developed for LEP [15] should help significantly.

We should like to make the following recommendations:

- The beam position monitor BPMH4120 must be added in the scheme.
- The corrector MDSV4003 can be dropped.
- The corrector MDGV4121 must be dropped.
- A study should be made whether it is possible to enforce the correction strength in the horizontal plane at the position of the MDMH4001, which we consider marginal.
- The two bending magnets MBHA and MBHC should be made available as correctors. They help significantly and reduced the required strength for the corrector MDMH4001.
- It should be investigated whether it is feasible to improve the monitoring system by adding monitors. While the effect of missing correctors can be partially compensated by clever correction strategies, the problem of missing monitors cannot be solved and could become critical under unlucky circumstances.

Alternatively, all presently foreseen monitors should measure the trajectory in both planes. Following some simulations, this is our preferred choice.

References

- [1] *The CERN neutrino beam to Gran Sasso*, Conceptual Technical Design, editor K. Elsener, CERN 98-02, INFN/AE-98/05, 19 June 1998;
- [2] *The CERN Neutrino beam to Gran Sasso (NGS)*, Addendum to report CERN 98-02, INFN/AE-98/05; CERN-SL/99-034(DI), INFN/AE-99/05;
- [3] *Update of changes to CNGS layout and parameters*, the CNGS project team, SL-Note-2002-012 EA;
- [4] *Fast extraction from SPS LSS4 for the LHC and NGS projects*, B. Goddard, SL-Note-98-066 SLI;
- [5] *The MKE Home Page*,(April 2002),
[http //uythoven.home.cern.ch/uythoven/Html/MKE/MKE_home.htm](http://uythoven.home.cern.ch/uythoven/Html/MKE/MKE_home.htm);
- [6] *Upgrade of the SPS Extraction Kickers for LHC and CNGS Operation*, J. Uythoven, E. Gaxiola, M. Timmins, to be published in the EPAC proceedings, Paris, May 2002;
- [7] *Design report of the MBG main bending dipoles for the proton transfer line TT41 to CNGS*; K.M. Schirm, SL-Note-2001-051 MS;
- [8] *Trajectory Correction of the LHC Injection Transfer Lines TI 2 and TI8*, A. Hilaire, V. Mertens, E. Weisse, LHC Project Report 122, June 1997;
- [9] *Analysis and optimisation of orbit correction configurations using generalised response matrices and its application to the LHC transfer lines TI 2 and TI 8*; Y.-C. Chao, V. Mertens, LHC Project Report 470, March 2001;
- [10] *Design report of the QTG quadrupoles for the CERN CNGS line*; Th. Zickler, SL-Note-2000-049 MS;
- [11] *The MAD-X Program*,(April 2002), info at: [http //cern.ch/MAD/](http://cern.ch/MAD/);
- [12] *Analysis and optimisation of orbit correction configurations using generalised response matrices and its application to the CNGS transfer line*, Y.-C. Chao, to be published.
- [13] *Technical specification for the MCIA resistive corrector dipole magnets for the TI 2 and TI 8 beam transfer lines*, D. Gerard, LHC Project document, to be published.
- [14] *Particle Accelerator Physics*, H. Wiedemann, Editor Springer-Verlag, Vol1, p.188.
- [15] *A New Closed Orbit Correction Procedure for the CERN SPS and LEP*, D. Brandt, W. Herr, J. Miles and R. Schmidt, Nucl. Instr. and Meth., **A293** (1990) 305.